Proceedings of ASME Turbo Expo 2025
Turbomachinery Technical Conference and Exposition
GT2025
June 16-20, 2025, Memphis, Tennessee

GT2025-153747

EXPERIMENTAL CHARACTERIZATION OF A MICRO GAS TURBINE FUELED BY AMMONIA-NATURAL GAS BLENDS

Chiara Anfosso
University of Genoa
Genova, Italy

Daria Bellotti
University of Genoa
Genova, Italy

Mario L. Ferrari
University of Genoa
Genova, Italy

Loredana Magistri
University of Genoa
Genova, Italy

ABSTRACT

Given the need to decarbonize the current energy production sector, to mitigate climate change and reduce greenhouse gas (GHG) emissions, innovative fuels are gaining increasing attention. In this context, ammonia represents a promising carbon-free energy carrier that can be used in energy storage, agriculture, transportation, and power conversion. This study focuses on an experimental analysis of a micro gas turbine (mGT) powered by various blends of natural gas and ammonia. The plant was developed within the framework of the FLEXnCONFU (FLEXiblize Combined Cycle Power Plants through Power-to-X Solutions using Non-CONventional Fuels) European project and is located at the Innovative Energy Systems laboratory of the University of Genoa. In this paper, the test rig, including the mGT retrofitting, fuel mixing system, and injection lines, is fully described, along with all the instrumentation required for control, measurement, and safety. The experimental campaign was conducted using different ammonia contents in the fuel blend at different mGT loads. The main operating mGT data (e.g., rotational speed, mass flow rate, injection pressure, turbine inlet, and outlet temperatures) that were acquired during the tests are presented and discussed. The measured results were used to develop an mGT performance map, which demonstrates the benefits of using ammonia in terms of total power production and CO_2 *reduction.*

Keywords: Micro gas turbine, ammonia, experimental campaign

NOMENCLATURE

CC	Combustion Chamber
FLEXnCONFU	FLEXiblize Combined Cycle Power Plants through Power-to-X Solutions using Non-CONventional Fuels
GHG	GreenHouse Gas
IES	Innovative Energy System
LHV	Lower Heating Value
MFC	Mass Flow Controller
mGT	micro Gas Turbine
SCR	Selective Catalytic Reduction
SOFC	Solid Oxide Fuel Cell
TIT	Turbine Inlet Temperature
TOT	Turbine Outlet Temperature

SYMBOLS

α	Parameter for pilot valve control [%]
β	Pressure ratio [-]
C_p	Specific Heat [kJ/kgK]
η_{Compr}	Compressor Isentropic Efficiency [-]
T_{amb}	Ambient Temperature [K]

1. INTRODUCTION

Due to the climate-neutral target imposed by the European Green Deal and the European Climate Law [1] and the related need to decrease CO_2 emissions, carbon-free alternative fuels are gaining increasing interest in the energy sector [2]. Moreover, the production of these fuels from renewable sources represents an important energy storage method to compensate for the fluctuations in power generation [3], such as those caused by day/night changes and weather conditions in solar systems [4][5]. In comparison with batteries [4], energy storage systems based on carbon-free fuel generation are expected to achieve higher energy density, reliability, and life [6]. For this reason, hydrogen, considered an interesting energy vector for its high efficiency and fast dynamics in PEM fuel cells, presents important limitations in terms of storability and transportability [7]. This is due to its low energy density in gaseous form (also at high-pressure conditions) and problems in terms of weight and costs in metal hydrides and liquified form [8]. Although liquid hydrogen is preferred in some applications (e.g. in aircraft) [9], it requires significant additional energy consumption to achieve and maintain cryogenic conditions. Considering these aspects, attention is also focused on other carbon-free fuels able to solve hydrogen's main application challenges [10]. Among different fuels considered for zero CO_2 emissions, liquid ammonia offers a higher hydrogen density than liquid hydrogen (i.e. 120

kgH_2/m^3 Vs 50 kgH_2/m^3), reducing generation and transportation costs (ammonia boiling temperature is about 240 K against about 20 K for hydrogen) [11]. Moreover, ammonia production is a well-established industrial process, mainly used in the fertilizer industry [12], and, due to similar physical characteristics to other commercial fuels, such as propane [13], existing infrastructure can be easily adapted for storage or transport.

Although ammonia can be directly used in Solid Oxide Fuel Cells (SOFCs) with high-efficiency conversion performance [14],[15], attention is also being directed toward ammonia combustors for potential integration with traditional power systems [16]. However, NH_3 as a fuel presents challenges, including slow flame speed in ammonia-air mixtures, difficulties with ignition, long ignition delays, a high auto-ignition temperature, and limited flammability range [17][18]. Moreover, high NO_X emissions are expected during ammonia combustion. Therefore, to face these issues, several studies have reported the development activities of combustors for burning ammonia or fuel blends including ammonia [19]-[23]. Moreover, due to growing interest in small-size systems for distributed generation, researchers have also started exploring ammonia utilization in micro gas turbines. In [24] a dedicated T100-based test rig is presented and used for steady-state tests with ammonia-methane blends, achieving up to 63% ammonia volumetric concentration. The test has been carried out by feeding only the main line with an ammonia-methane blend and values up to 2000-2500 ppmvd (15% oxygen concentration) of NO_X have been measured. In [25], Toyota developped and successfully tested a combustor for its 300kW mGT starting from the already existing one designed for LNG. With the new combustor, Toyota carried out an experimental test where the mGT, started with 100% LNG, was gradually able to achieve 100% ammonia combustion. However, despite the increasing interest in micro gas turbines powered by ammonia or ammonia blends, the development of experimental test rigs remains very limited, and data on their impact on gas turbine performance (e.g., pressure ratio, rotational speed, temperatures) and dynamic behavior are scarce in the literature. Therefore, the work here presented investigates the experimental performance of a mGT operating on various blends of natural gas and ammonia and various loads. The activity has been carried out in the framework of the FLEXnCONFU [26] (FLEXiblize Combined Cycle Power Plants through Power-to-X Solutions using Non-CONventional Fuels) European project and the test-rig has been developed by the Innovative Energy Systems (IES) laboratory of the Thermochemical Power Group, University of Genoa. A T100-mGT was specifically retrofitted with the installation of a new combustion chamber designed for the combustion of low-LHV fuel blends and equipped with several thermocouples to measure the temperature distribution within the component, providing data for further optimization and validation of computational models. Additionally, a custom fuel system was integrated, and the control system of the machine was modified accordingly. Compared to commercial machines, the test rig features modifications and additional instrumentations for measuring mass flow rates, pressures, and temperatures across the T100 components [27]. Furthermore, in addition to what has been reported in the literature, the experimental campaign was conducted testing different natural gas–ammonia fuel blends at different mGT loads, enabling the development of a detailed machine mapping. Additionally, transient condition tests were conducted to evaluate the impact on the T100 control system.

2. TEST RIG

The test rig used in this activity is based on the T100 micro-gas turbine available in the IES laboratory [27] and used in previous works for the emulation of hybrid systems including a SOFC [28]. For the tests presented here, the external vessels and the related devices were disconnected, to operate on the T100 microturbine in its standard layout.

2.1 T100 micro-gas turbine

The T100 microturbine is a commercial recuperated gas turbine able to produce 100 kW net electrical power in nominal conditions, fed by natural gas. Since the machine installed in the laboratory is a PHS Series 3 version, it is also equipped with a heat exchanger to produce hot water for cogeneration, partially harvesting the heat in the exhausts. TABLE 1 reports the nominal values for the main T100 properties, as from [29].

TABLE 1: T100 MAIN PARAMETERS IN NOMINAL CONDITIONS

Property	Nominal value	Unit
Net electrical generation	100 ± 3	kW
Fuel Power	333	kW
Electrical efficiency	30 ± 1	%
Turbine Outlet Temperature	645	°C
Pressure ratio (β)	4.5	-
Rotational speed	70,000	rpm
NOx emissions @ 15% O2, 100% load, 15°C air temperature	≤15	ppm
CO emissions @ 15% O2, 100% load, 15°C air temperature	≤15	ppm

Since this microturbine was modified including connections with an external volume, not used in this work, but described in [29] for details, it is not able to reach nominal rated conditions. This limitation is due to the additional pressure losses (including those between the compressor outlet and the turbine inlet) and the higher-than-expected intake air temperature, which remains above 25°C even during winter tests. This is due to the laboratory setup and the modifications made (including long additional external pipes that, even if equipped with insulation, release heat to the environment due to temperature values in the 600°C range) [28][29]. For these reasons, the maximum net electrical power that can be produced with this T100 machine is about 70 kW at 70,000 rpm.

2.2 New fuel line

The test rig presented in this work has been specifically developed to enable the feeding of the mGT with various ammonia-based fuel mixtures. To achieve this, four separate fuel lines have been implemented for H_2, N_2, NG, and NH_3. This setup provides the flexibility to create a range of fuel blends, including natural gas-ammonia mixtures as well as combinations of hydrogen, nitrogen, and ammonia, simulating various levels of ammonia cracking. This capability is crucial for testing fuel blends with different compositions, including those achieving a zero-carbon footprint.

To accommodate this functionality, the original commercial fuel system integrated into the T100 microturbine was disconnected, and a series of custom components were installed to handle the new fuel configurations. The detailed P&ID of the injection system, outlining its design and operation, is shown in FIGURE 1. All the lines and fittings are made of stainless steel AISI 316, and the seals are made of Teflon or EPDM to be suitable for use with ammonia.

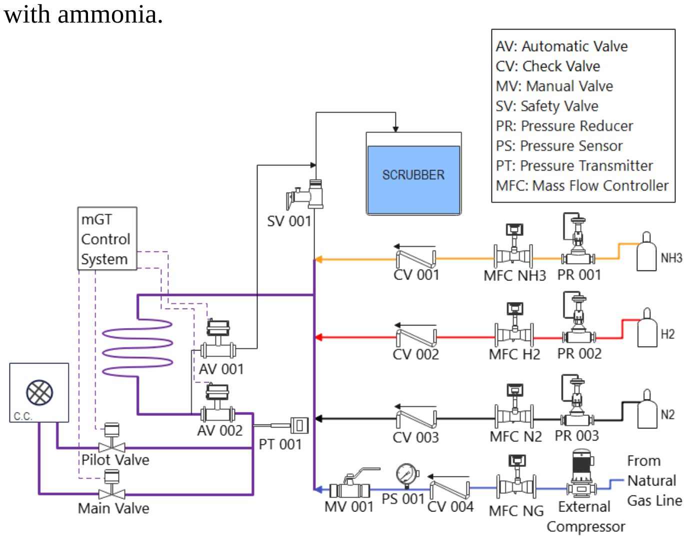

FIGURE 1: NEW FUEL LINE P&ID

In detail, instead of utilizing the original onboard compressor, an external system was implemented to provide a fully controllable natural gas flow at a nominal pressure of approximately 7 bar. Hydrogen and nitrogen are supplied from high-pressure cylinders stored at 200 barg, necessitating the use of pressure reducers on both lines to regulate the flow. The laboratory is equipped with 32 and 6 hydrogen and nitrogen cylinders, respectively. Ammonia is also supplied from bottles; however, due to national regulations, no more than 75 kg of ammonia can be stored in the IES laboratory. To comply with these restrictions, three 20 kg ammonia bottles are used to feed the mGT during the experiments.

To address the cooling effect that occurs when gaseous ammonia is extracted from the bottles, causing a temperature drop in the remaining liquid portion, a temperature-controlled heating process is employed. This system exploits thermal energy produced by the mGT operated in cogenerates mode to facilitate the evaporation of liquid ammonia, ensuring a consistent and stable gas flow for tests. The temperature is controlled by adjusting the amount of exhaust gases that bypass the mGT heat exchanger. Moreover, all the lines are equipped with mass flow controllers, and, to enable the blending of ammonia with other gases, a 1-inch diameter pipe with multiple inlets is used. After the blending, the gas mixture enters in a 12-meter coil with a 1-inch diameter which is necessary to decouple the dynamics of the controllers from the operation of the T100 fuel valves (for the management of the pilot and the main lines at the combustor inlet level). Finally, a safety valve was installed to prevent overpressure conditions. In case of fuel overpressure and during the T100 shutdown phases the blend is driven to a water-based scrubber and discharged to the environment in a safe zone exploiting the high solubility of ammonia in water. Lastly, the original mGT injection valves (pilot and main), originally made of brass, were replaced with stainless steel valves for ammonia compatibility.

TABLE 2 outlines the specifications of the instruments installed in the plant.

TABLE 2: INSTRUMENTS SPECIFICATIONS

Description	Accuracy	Model
Mass Flow Controller (MFC)		
Natural gas flow controller	±1.5%	Burkert Type 8746
Hydrogen flow controller	±1.5%	Burkert Type 8746
Nitrogen flow controller	±1.5%	Burkert Type 8746
Ammonia gas flow controller	±1.5%	Burkert Type 8746
Valves		
Hydrogen pressure regulator	N/A	FAIG Model VSPGC
Nitrogen pressure regulator	N/A	FAIG Model VSPGC
Ammonia pressure regulator	N/A	FAIG Model VSPGS
AV002 mGT feeding valve	N/A	Habonim C15 SR-2 MET
AV001 release to storage tank	N/A	Habonim C15 SR-2 MET
Pilot valve	±0.5%	Burkert type 2875
Main Valve	±0.5%	Burkert type 2875
Check valves		
One on each branch	N/A	FITOK Type 316 ASTM A479
Safety Valve		
Overpressure valve	N/A	N. G.I. model VX6D10/CS-1/2
Pressure Sensor		
PT 001 (0-10 bar)	±0.5%	IMI Norgren 34D-V101G-DD1-AA
Thermocouples		
TOT and CC	±2.5 K	Type K
TIT	±1.5 K	Type N
Gas Analyzer		
NO and NO_2 measured at the mGT exhaust outlet	±5 ppm	Seitron Chemist 900

2.3 NEW COMBUSTION CHAMBER

Operating the T100 with fuel blends that have a lower calorific value than natural gas requires an increased fuel/air ratio to ensure more stable combustion. Based on the similar Wobbe Index of ammonia and biogas, the mGT retrofitting involved using the combustion chamber developed by Ansaldo Green Tech for biogas applications. This adaptation includes larger dilution holes and fuel nozzle orifices compared to the natural gas-based combustion chamber.

Moreover, to keep under control some critical parameters of the machine, the new chamber was equipped with a series of temperature transducers located all along the burner as depicted in FIGURE 2: i) 3 thermocouples (type K) are located on the combustor liner ii) other 3 thermocouples (type K) are located on the liner on the opposite side (180°) iii) 2 thermocouples (type N) are located at the end of the liner to measure the Turbine Inlet Temperature (TIT) iv) 3 thermocouples (type K) are located at different depth and equally spaced (120°) of the pilot flame pipe. FIGURE 3 and FIGURE 4 show the fuel mixing system and the new combustor installed in the microturbine, respectively.

FIGURE 4 highlights the main and pilot fuel valves and injection lines, as well as the spark plug placement area. FIGURE 3 features the mass flow controllers, the overpressure safety valve, the mixer, and the coil, as detailed in the P&ID from FIGURE 1.

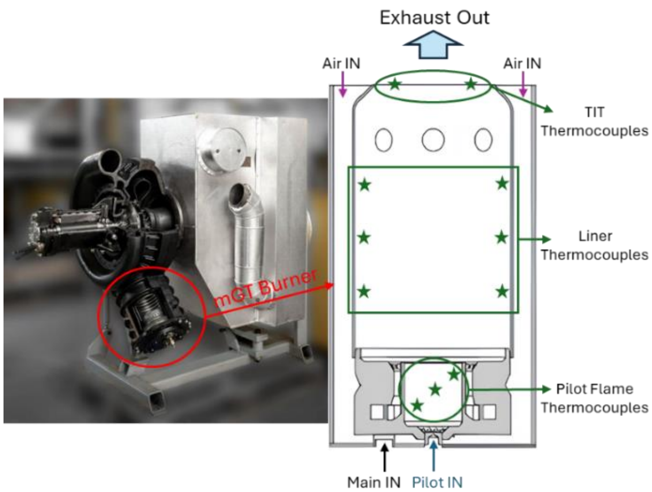

FIGURE 2: THERMOCOUPLE POSITIONS IN THE NEW COMBUSTION CHAMBER

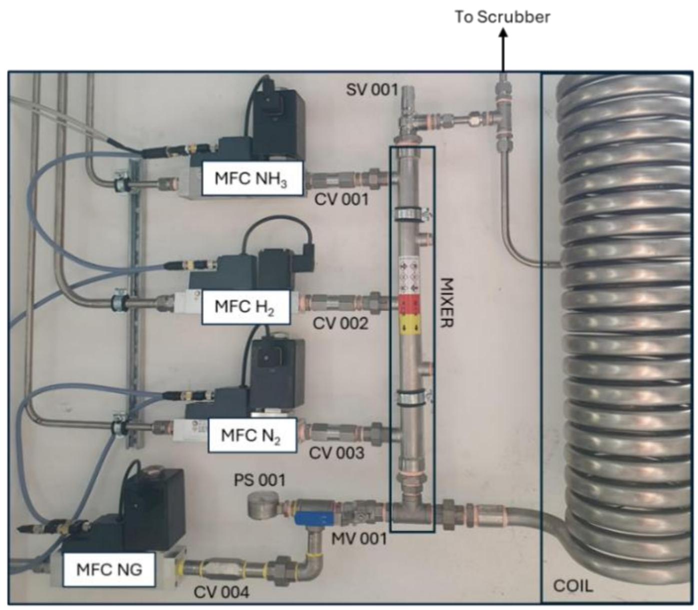

FIGURE 3: NEW T100 FUEL INJECTION LINE

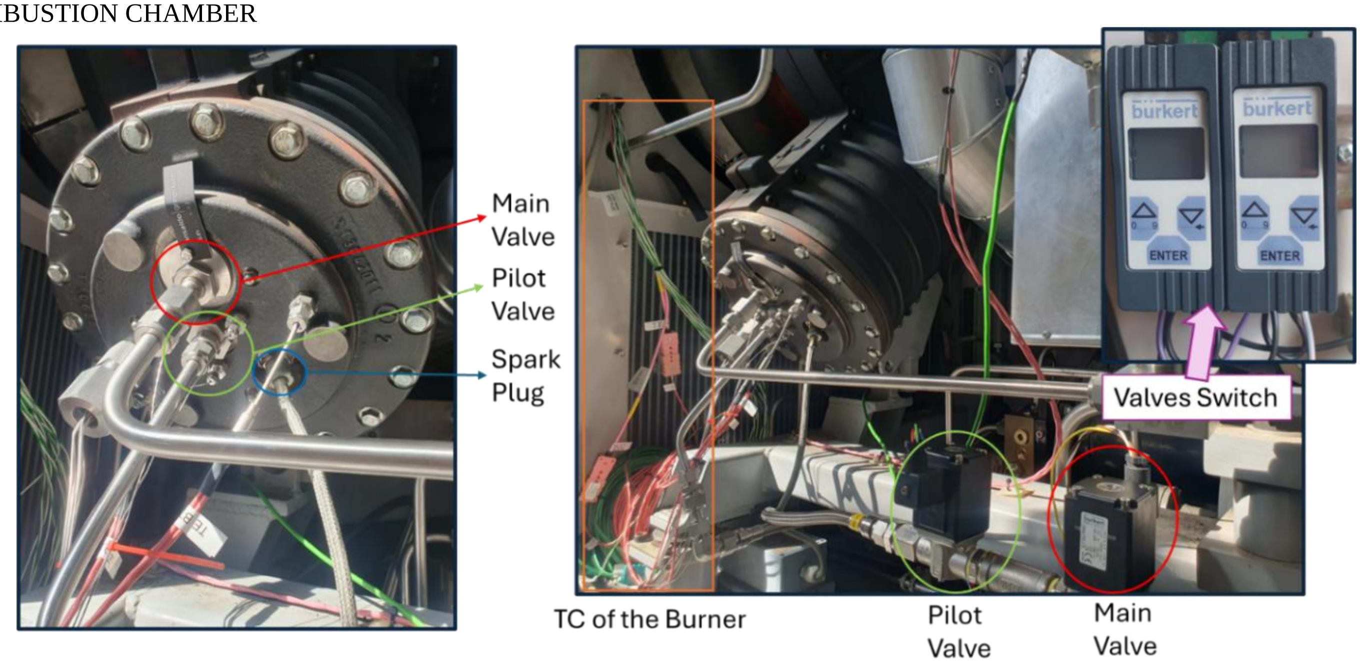

FIGURE 4: NEW T100 COMBUSTION CHAMBER

2.4 New mGT Control System

The original mGT control system, when the turbine is operating at low power, maintains constant the rotational speed at the minimum values of 50,000 rpm, increasing the TOT (*n* control state). As soon as the TOT reaches 645°C, the control system starts to maintain constant the temperature, increasing the rotational speed (TOT control state).

The existing control system was modified by the manufacturer to increase the level of flexibility and the control number variables allowing different fuel flow split between the pilot and main line. Specifically, the control logic in terms of *n* control state and TOT control state has been maintained, however, the system now enables real-time adjustment of the standard pilot contribution for each combination of speed and TOT by introducing a parameter (α). This parameter is used to scale the pilot valve opening percentage that the control system sends to the fuel valve control card (Valves Switch in FIGURE 4). The main line contribution depends on the pilot line, and since the opening percentage of both valves is influenced by the Lower Heating Value (LHV) of the fuel, and different fuel blends need to be used, an adjustable variable for the LHV was implemented (for modifications throughout the tests).

3. RESULTS AND DISCUSSION

The development of the previously described test rig was completed in June 2024, marking the start of the experimental test campaign during the summer of the same year. The campaign is ongoing, and this section aims to present the main results achieved thus far with the retrofitted mGT operating on various blends of ammonia and natural gas. The presented findings focus on understanding the behavior of the mGT, including its efficiency, emissions, and control system adaptability.

The work also involves characterizing the new combustion chamber with traditional fuels. This evaluation aims to assess the performance and stability of the chamber and its impact on the mGT control system. The goal is to ensure that retrofitting does not compromise the turbine's overall operation or dynamic response. Additionally, the data collected during the campaign were utilized to create mGT maps based on the load and ammonia concentration. These maps also incorporate the pressure ratio (β) and the airflow processed by the compressor, enabling the determination of the compressor operating point and an assessment of the surge margin.

3.1 Natural Gas tests: mGT characterization with the new combustion chamber

The experimental test campaign was initially carried out with only natural gas to set the reference condition of the microturbine equipped with the new Combustion Chamber (CC). The startup phase was evaluated, along with the injection valves' opening percentage as it varied according to the mGT load. FIGURE 5 shows, in terms of *rpm*, that no significant variation during start-up with natural gas is measured: the trend and timing have remained almost unchanged.

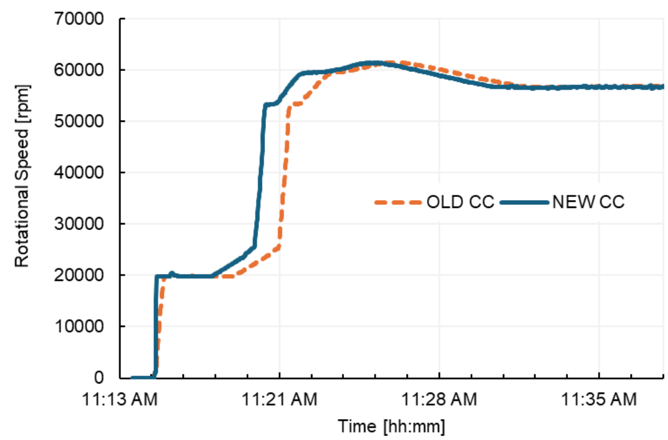

FIGURE 5: ROTATIONAL SPEED DURING START UP in 100% NG: OLD VS NEW COMBUSTION CHAMBER

FIGURE 6 reports the fuel valves opening percentage at different mGT loads from 20 kW to 50 kW for the "OLD CC" and "NEW CC" configurations, respectively. It is noticeable that the transient phases in the load ramp are even more stable with the new CC, particularly for loads ≤ 40 kW. Additionally, while the pilot valve opening percentage remains nearly the same in both configurations, the main valve is 3% more closed when using the new combustion chamber.

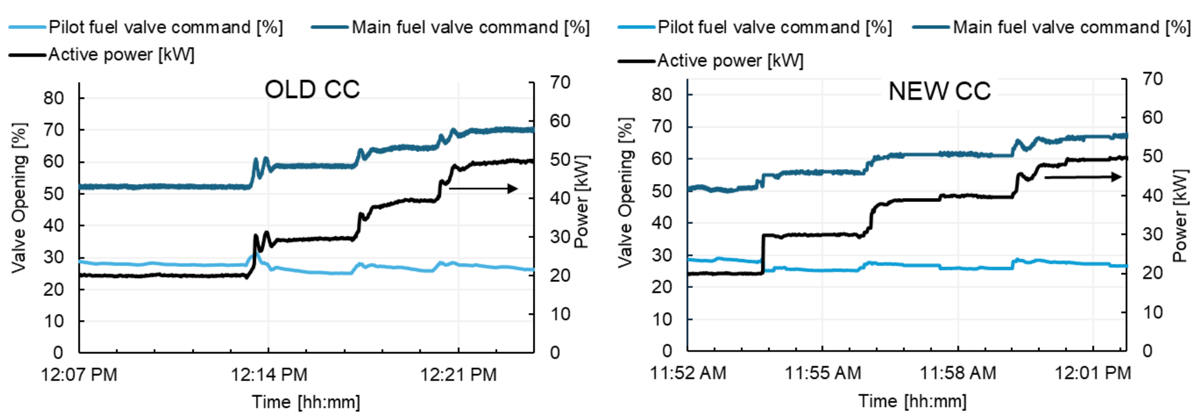

FIGURE 6: VALVE OPENING AND POWER PRODUCTION DURING T100 LOAD RAMP: OLD VS NEW CC (100%NG)

Regarding NOX emissions, FIGURE 7 presents the reference baseline, showing the recorded values from the micro gas turbine's minimum load to its maximum load.

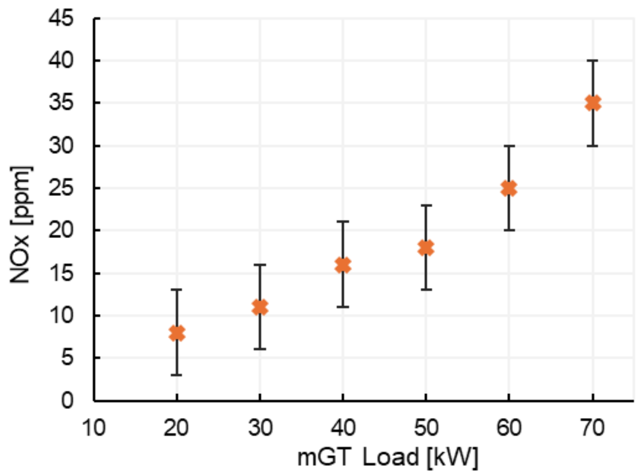

FIGURE 7: NOx FORMATION WITH THE NEW CC

3.2 Ammonia-Natural Gas blends: test results

To evaluate the impact of injecting ammonia in the T100, experiments were conducted starting with natural gas and reaching the desired mGT net electrical power output. Then, ammonia was gradually injected. All experiments were conducted by controlling the ammonia flow through the MFC_{NH3}, while the MFC_{NG} was kept fully open at 100%. This approach was chosen because operating with only two fuels allows the mGT, once the target power is set and the ammonia supply is controlled, to automatically adjust the natural gas flow to compensate for the difference between the target thermal input and the amount provided by the ammonia. Therefore, the natural gas mass flow rate is controlled by the mGT to reach the target power set by the user. Different tests with ammonia/natural gas blend have been performed and the maximum amount of ammonia injected into the mGT as well as the operative power range is reported in TABLE 3.

TABLE 3: TEST MATRIX (YEAR 2024)

Date	Max NH_3 [m/m]	mGT Power range [kW]
Aug. 6th	20%	20-30
Sept. 3rd	18%	25
Sept. 3rd	20%	25-70
Sept. 9th	41%	35
Sept. 17th	34%	40
Sept. 30th	40%	40
Oct. 15th	39%	60-70
Oct. 15th	52%	40
Oct. 23th	40%	50
Oct. 23rd	63%	30-50

This section presents three test results (TEST 1, TEST 2, TEST 3) which have been considered particularly significant in providing information on both mGT dynamic behavior as well as critical aspects that emerged during the campaign. TEST 1 and 2 have been carried out on October 15th whereas TEST 3 is the last one reported in TABLE *3*.

TEST 1 involved operating the microturbine to maximum load and then injecting ammonia up to the maximum admissible value without utilizing the ammonia heating system. TEST 2, was conducted at a lower power target (57% load) with the goal of verifying the turbine stability even with ammonia content higher than that of natural gas. TEST 3 reports the results achieved with a maximum of 63% m/m of ammonia with the mGT operating under challenging conditions (i.e., with low fuel injection pressure).

3.2.1 TEST n.1

The initial test involved bringing the mGT to 100% load and then injecting ammonia up to the maximum admissible value. FIGURE 8 shows the flow rates of natural gas and ammonia, along with the actual electrical power output of the mGT. As ammonia injection begins, the natural gas flow decreases, while the power production consistently meets the set point. When the ammonia injection exceeded 39% m/m (around 3:43 PM), it became impossible to extract additional gaseous ammonia due to the excessively low temperature of the liquid phase. Therefore, the power target was adjusted to 60 kW to evaluate also the dynamic behavior of the mGT, in the meanwhile, ammonia content was reduced. The ramp-down is quick, and from an electrical power perspective, the mGT handles the transition smoothly and stably.

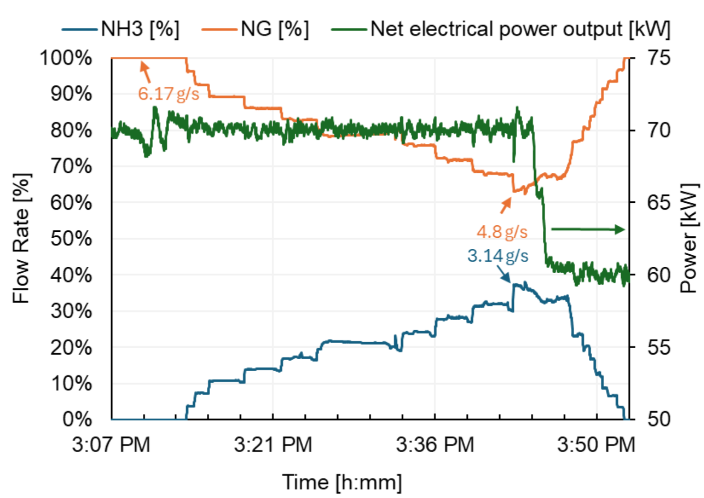

FIGURE 8: FLOW RATES AND POWER PRODUCTION (TEST 1)

Stable operation is further confirmed by examining the rotational speed and TOT (FIGURE 9). The control system maintains the TOT constant at 645°C, while the speed is adjusted to accommodate the reduction in electrical power output.

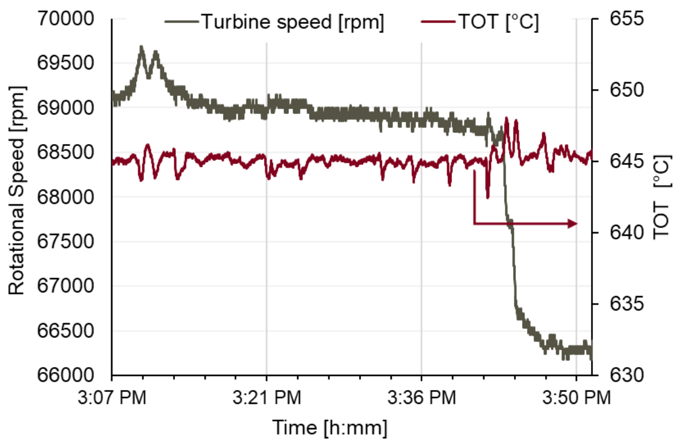

FIGURE 9: ROTATIONAL SPEED AND TOT (TEST 1)

From an efficiency standpoint, the introduction of ammonia leads to a reduction of about 2% (FIGURE 10). This outcome depends on several factors (i.e., lower pressure ratio, lower rotational speed and lower air flow rate) but it is also directly linked to the higher specific heat (c_p) of the mixture. While this characteristic allows for a greater enthalpy difference in the turbine, it also means that the gas requires more energy to be heated in the combustion chamber. As a result, more thermal energy is needed to achieve the same temperature difference within the combustion chamber [30]. Although the values are not exactly the same due to differences in system and operating conditions, the decreasing trend in efficiency with increasing ammonia content aligns with the results reported in the experimental study by Avila et al. [24] and the theoretical studies carried out by the authors [30] and by Bonasio et al. [31].

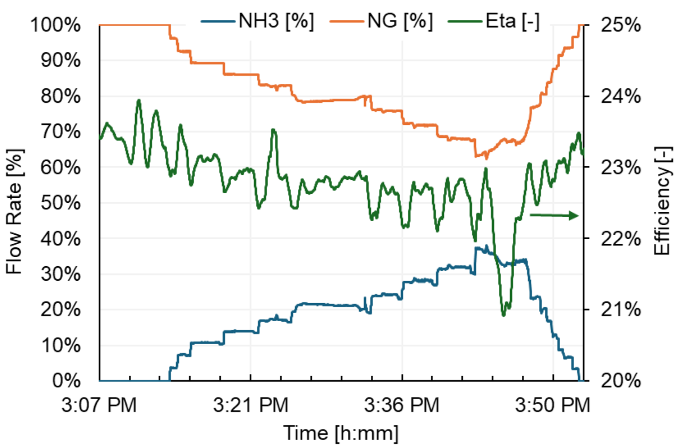

FIGURE 10: FLOW RATES AND EFFICIENCY (TEST n.1)

The analysis of the temperature inside the combustion chamber revealed some interesting findings: there are no significant variations when ammonia is injected, except for the pilot flame thermocouple labeled "T primary swirler inner top" in FIGURE 11. This temperature is measured in the pilot zone at the position closest to the main combustion zone. When reaching 37% ammonia, the temperature drops by nearly 350°C, stabilizing at around 620°C. This indicates that the flame has detached from its initial position and shifted toward the outlet of the combustion chamber. In this sense, efforts are currently also focused on developing a detailed CFD model to analyze the temperature and velocity fields at every point within the combustion chamber for various ammonia-natural gas blend compositions.

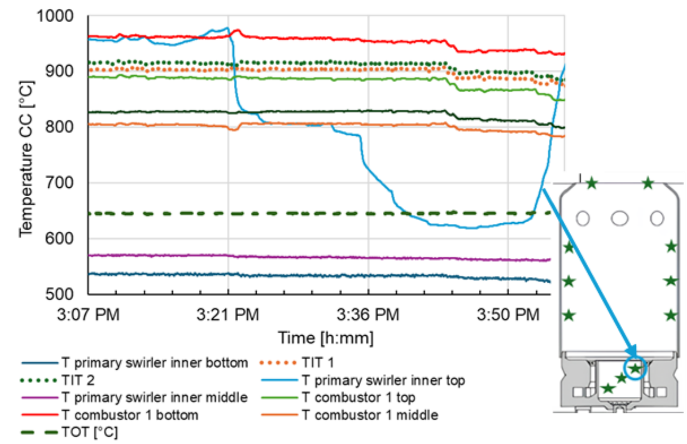

FIGURE 11: TEMPERATURE PROFILE INSIDE THE COMBUSTION CHAMBER (TEST 1)

3.2.2 TEST n.2

The second test was conducted at a lower power target, specifically maintaining the mGT at 40 kW. In this test, a larger proportion of ammonia was injected, exceeding 50% m/m. The objective remained to verify the turbine stability even with ammonia content higher than that of natural gas, as shown in FIGURE 12. Additionally, unlike the previous test, ammonia was injected rapidly, requiring the mGT to respond swiftly with adjustments in the injection valve opening to maintain a consistent thermal input.

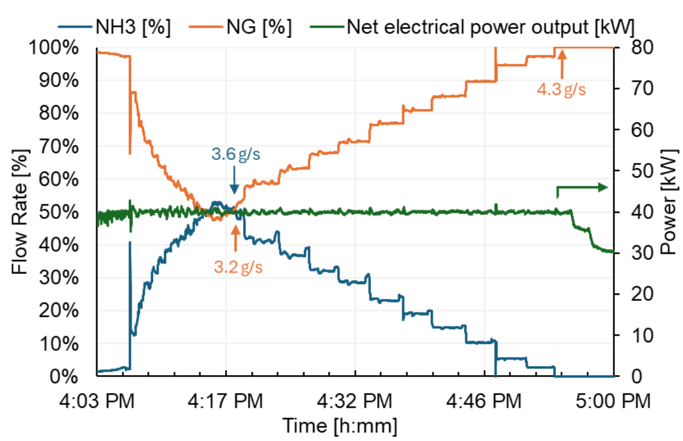

FIGURE 12: FLOW RATES AND POWER PRODUCTION (TEST n.2)

As illustrated in FIGURE 13, as ammonia injection increases, the main valve opens to nearly 72%. This is primarily because a higher volumetric flow rate is needed to maintain consistent power output. Additionally, it can be observed that the injection pressure slightly rises to compensate for the higher-pressure losses occurring in the injection valves during the transition phase.

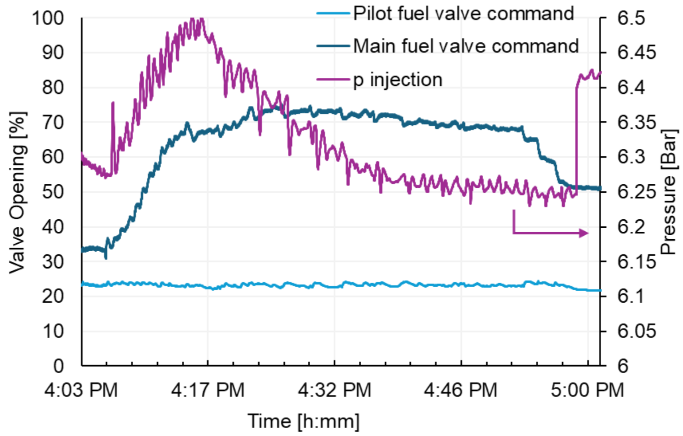

FIGURE 13: VALVE OPENING PERCENTAGE AND INJECTION PRESSURE (TEST 2)

The test also confirmed that, even with higher levels of ammonia, the mGT successfully maintained a constant TOT at approximately 645°C and a stable rotational speed around 62,250 rpm as depicted in FIGURE 14.

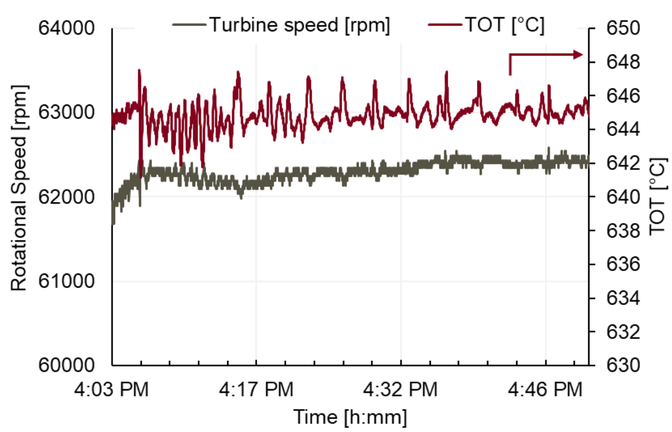

FIGURE 14: ROTATIONAL SPEED AND TOT (TEST n.2)

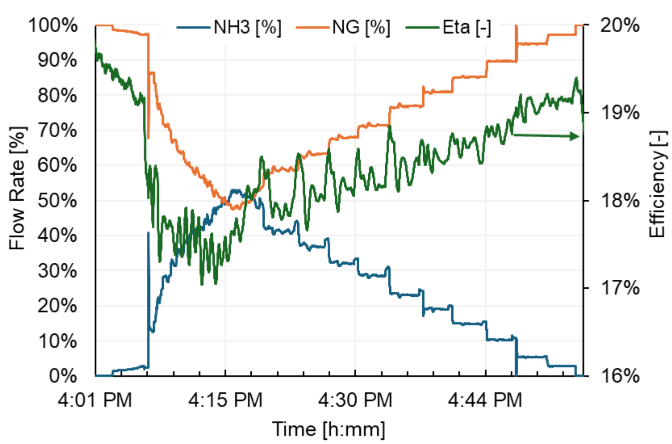

FIGURE 15: FLOW RATES AND EFFICIENCY (TEST n.2)

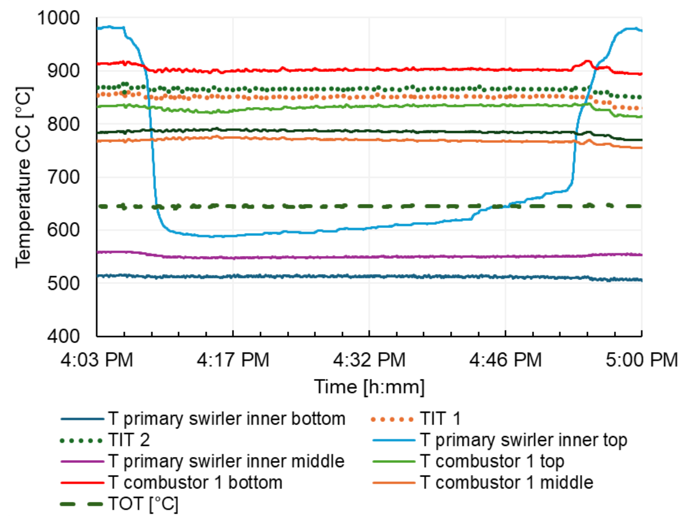

FIGURE 16: TEMPERATURE PROFILE INSIDE THE COMBUSTION CHAMBER (TEST n.2)

In this case, as well, efficiency decreases by almost 2% when ammonia is used (FIGURE 15), and the temperature measured at the outlet of the pilot flame zone drops significantly (FIGURE 16). However, since the amount of ammonia in the CC is higher than in the previous test, the temperature settles at around 590°C, indicating that the flame has detached even further from its original position. From the emissions perspective, FIGURE 17 reports the results achieved with the mGT running at 40 kW. The obtained values are in line with those reported by Avila et al. [24], and the significant impact of NO_X emissions is further confirmed by the experiments conducted by AIST [32]. However, the values from AIST are not directly comparable due to the use of a very different system in their study compared to this work. Thus, while there is a significant reduction in CO_2 emissions (-19.5%, equivalent to 0.86 $kgCO_2/kWh$), NO_X levels increase dramatically, reaching 2208 ppm, comprising 1956 ppm of NO and 252 ppm of NO_2. It should also be emphasized that for each ammonia flow rate, no unburned ammonia was detected.

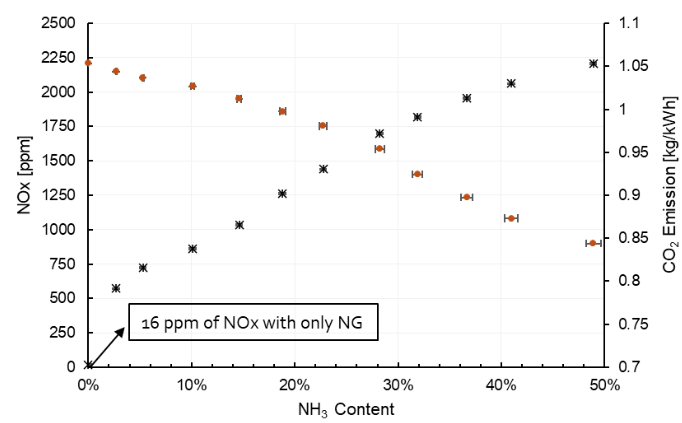

FIGURE 17: NO_X AND CO_2 EMISSIONS AT 40 kW

In summary, the results presented so far demonstrate that injecting ammonia into a commercial mGT, following a retrofit focused on the combustion chamber, is feasible and maintains turbine stability. Furthermore, the decrease in temperature in the pilot flame zone suggests a reduced risk of flashback. This is associated with the lower adiabatic flame temperature and flame velocity of the mixture. From the perspective of conducting tests with fuel blends produced from the ammonia partially cracking process, the presence of ammonia is desirable as it counteracts the high velocity and temperature of the hydrogen flame, enabling the mGT to operate safely and stably.

Moreover, a blend of 50% ammonia leads to a substantial reduction in CO_2 emissions. However, as a drawback, an additional NO_X reduction system must be integrated due to the significant increase in NO_X levels. As proven by AIST in their 50kW mGT [32], the integration with a SCR system could lead to a NO_X reduction of 95%. If the same reduction would be applied to the microturbine analyzed in this study, values of NO_X lower than 110 ppm could be achieved.

Another noteworthy aspect that emerged from the experimental campaign is the formation of ammonium carbonate $(NH_4)_2CO_3$ presumably due to the interaction between ammonia, H_2O and CO_2 in the natural gas at ambient temperature and ~6 bar. Domestic natural gas, in fact, contains impurities such as CO_2 and H_2O, which could react with ammonia to produce ammonium carbonate according to the reaction (1).

$$2NH_3+CO_2+H_2O \rightarrow (NH_4)_2CO_3 \quad \Delta H = 37.9 kJ/mol \qquad (1)$$

The reaction typically occurs at moderate temperature (10 – 50°C) and low pressure (i.e. 1 - 6 bar) which align with the operating range reported in this test. However, while this explanation appears plausible, further verification is required to confirm the actual mechanism of ammonium carbonate formation.

FIGURE 18 shows a section of the fuel pipe after 1 hour and 3 hours of testing the system with ammonia and natural gas blends. As shown, the formation of ammonium carbonate is significant, leading to a substantial reduction in the flow passage area that in turn causes a significant pressure drop as can be observed in FIGURE 19.

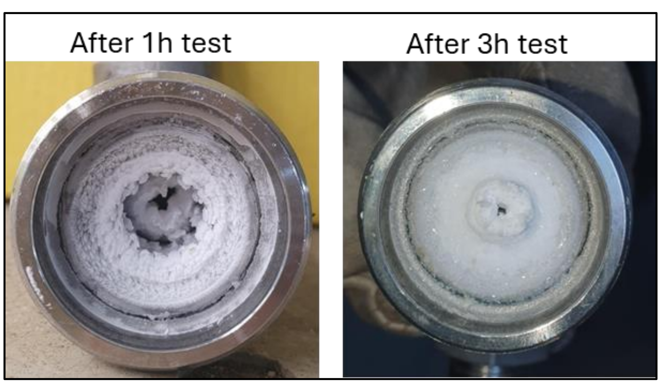

FIGURE 18: AMMONIUM CARBONATE FORMATION DURING EXPERIMENTAL TESTS

The formation rate of $(NH4)_2CO_3$ has been roughly estimated at approximately 10 g/h. Based on calculations, to produce this amount of ammonium carbonate with the mGT operating at 40 kW, a concentration of 130 ppm of H_2O and 318 ppm of CO_2 in the natural gas would be sufficient. These impurity levels adhere to national regulations, which specify maximum allowable concentrations of 2500 ppm for CO_2 and 1000 ppm for H_2O in natural gas intended for domestic use [33].

This aspect must be carefully considered when continuously fueling the mGT with such a blend. To address this issue, one possible option is to install a drying unit to completely remove H_2O contained in the natural gas stream. However, achieving a fully dry mixture could be complex and costly. Another solution could be operating within a temperature range that inhibits ammonium carbonate formation (i.e. at atmospheric pressure, this would require installing a heating system to keep the mixture above 58°C). If the second option is chosen and the mGT can operate in CHP mode, the heat needed for reaction inhibition could be directly supplied by the mGT.

3.2.3 TEST n.3

FIGURE 19 illustrates that when the ammonia content in the mixture reaches approximately 45% m/m, the injection pressure drops significantly due to the continuous reduction of the flow passage section caused by increased carbonate formation. Even after the ammonia is removed from the system, the pressure does not return to its initial value but stabilizes at 1.8 bar lower due to the reduced section. It is important to note that this test was conducted following a previous one, meaning that ammonium carbonate was already present inside the pipeline at the start of the test. When the pressure begins to drop, the mGT can no longer maintain the original 50 kW setpoint, resulting in a decline in power output, as shown in FIGURE 20. With this level of ammonia and the reduced flow section, the pilot valve was opened to 33%, while the main valve reached 94%.

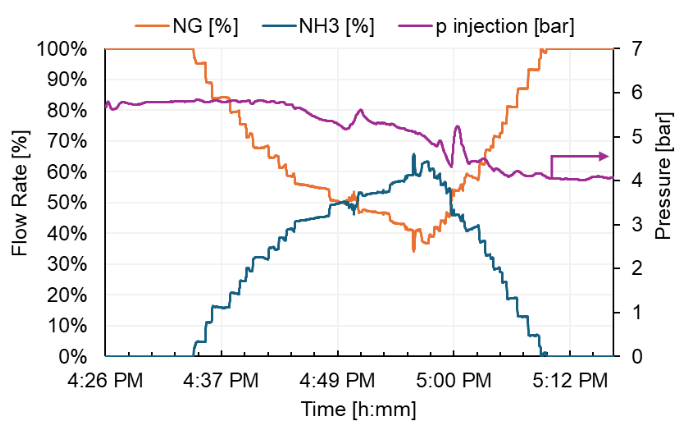

FIGURE 19: FLOW RATES AND INJECTION PRESSURE (TEST n.3)

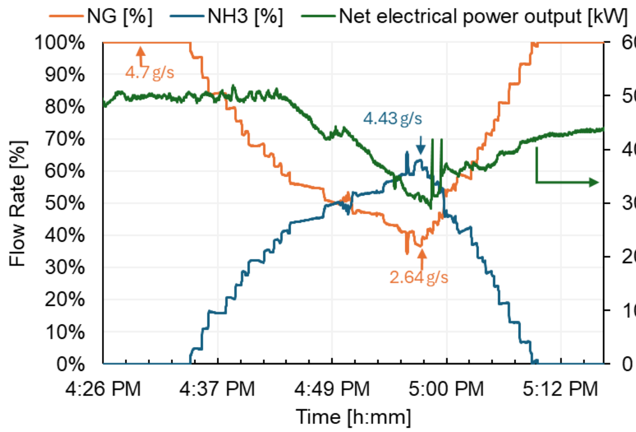

FIGURE 20: FLOW RATES AND POWER PRODUCTION (TEST n.3)

Under these unfavorable conditions, the mGT control system maintained the TOT within a range around 645°C by adjusting the shaft speed, although greater fluctuations were observed compared to the other two tests discussed in this study (as reported in FIGURE 21).

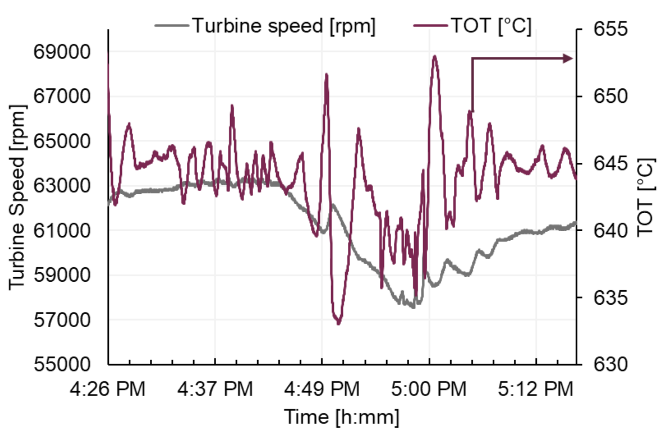

FIGURE 21: ROTATIONAL SPEED AND TOT (TEST n.3)

Therefore, the mGT can handle high levels of ammonia blended with natural gas, even under challenging conditions. However, to prevent significant reductions in flow section, it is essential to pretreat the natural gas, (including domestic gas, which was used for these tests), before mixing it with ammonia or, as previously mentioned, to operate within a temperature range that inhibits ammonium carbonate formation.

3.3 mGT characterization

The results achieved during the experimental campaign have been used to characterize the mGT in terms of rotational speed, efficiency, pressure ratio and air mass flow rate shown in FIGURE 22, FIGURE 23, FIGURE 24, and FIGURE 25 respectively. The values reported in the graphs are based on the average data obtained during mGT operation under those specific conditions. The mean is calculated using a minimum of 60 points and a maximum of 300 points, depending on the case.

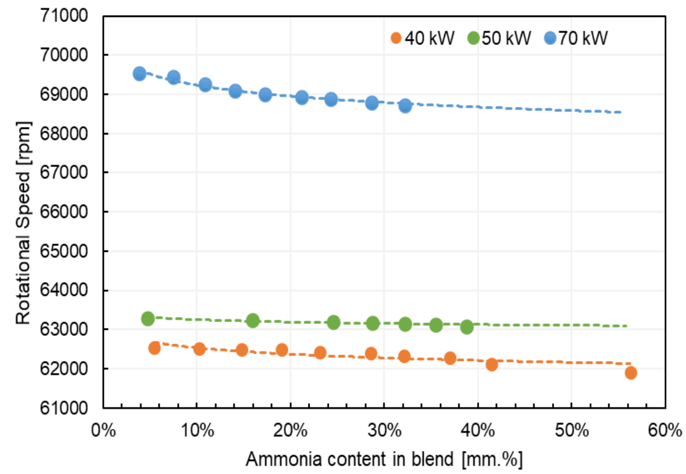

FIGURE 22: mGT ROTATIONAL SPEED AS FUNCTION OF POWER PRODUCTION AND NH_3 CONCENTRATION

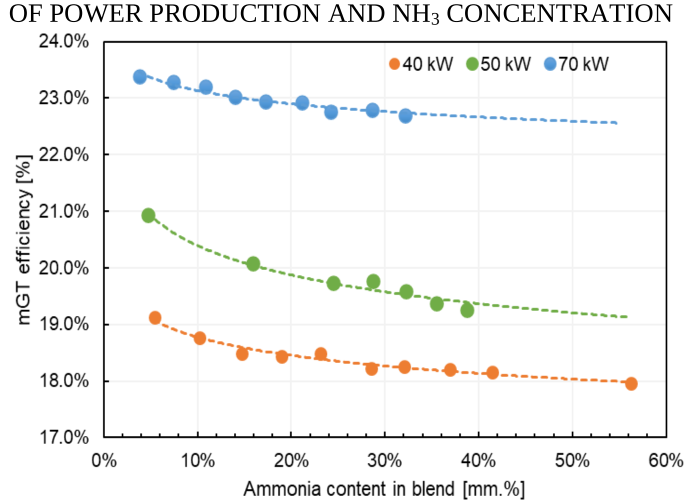

FIGURE 23: mGT EFFICIENCY AS FUNCTION OF POWER PRODUCTION AND NH_3 CONCENTRATION

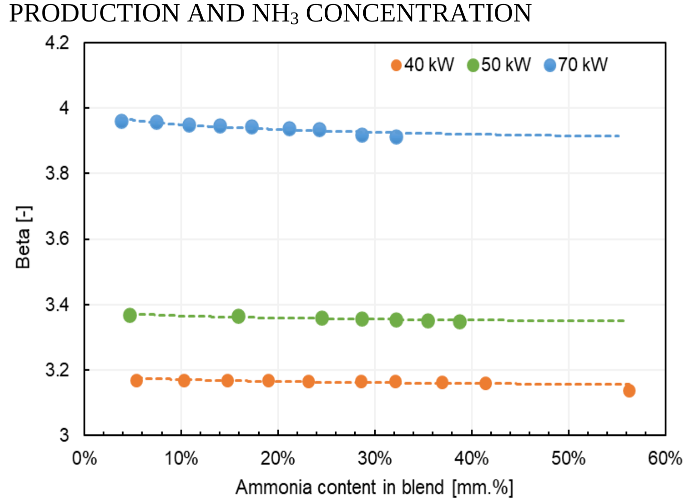

FIGURE 24: mGT PRESSURE RATIO AS FUNCTION OF POWER PRODUCTION AND NH_3 CONCENTRATION

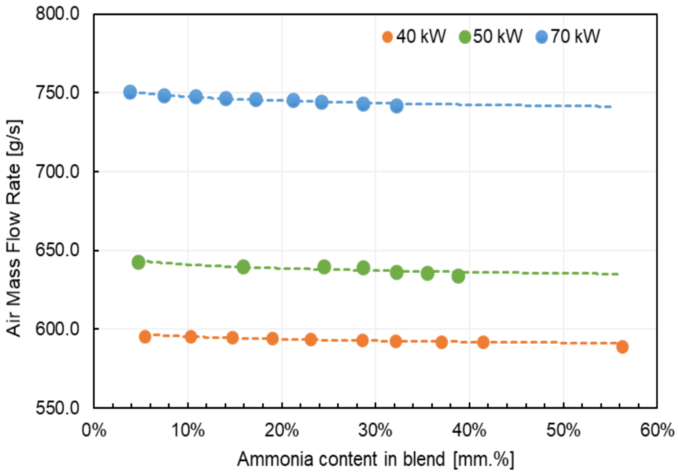

FIGURE 25: mGT AIR FLOW AS FUNCTION OF POWER PRODUCTION AND NH_3 CONCENTRATION

Increasing the NH_3 content enables operation at a lower rotational speed, which in turn allows the mGT to achieve greater power output. Additionally, using an ammonia blend requires a lower β due to the increased fuel injection needed in the combustion chamber. Consequently, the mass flow rate processed by the compressor is reduced. This is attributed to the combined effects of the lower rotational speed needed for a given power output, the reduced pressure ratio, the higher heat capacity of the flue gases [30], and the decreased specific work required by the compressor.

The compressor work (W_{Compr}) is, in fact, calculated as (2) and from FIGURE 26 it can be seen that operating with ammonia, allows the compressor to operate also at higher isentropic efficiency (η_{Compr}).

$$W_{Compr} = \frac{C_p * T_{amb} * \left(\beta^{\frac{\gamma-1}{\gamma}} - 1\right)}{\eta_{Compr}} \qquad (2)$$

FIGURE 26 illustrates the compressor operating points for various power outputs (40 kW, 50 kW, and 70 kW) of the mGT, comparing operation with pure natural gas (traditional configuration) to ammonia-natural gas blends. FIGURE 26 also highlights that operating with ammonia does not increase the risk of surge, as the operating points shown remain well within a safe distance from the surge margin SM (1.386, 1.404, and 1.415 for 40 kW, 50 kW and 70 kW respectively). The SM is calculated as (3):

$$SM = \frac{\frac{\beta_{surge}}{\dot{m}_{air,corrected,surge}}}{\frac{\beta}{\dot{m}_{air,corrected}}} \qquad (3)$$

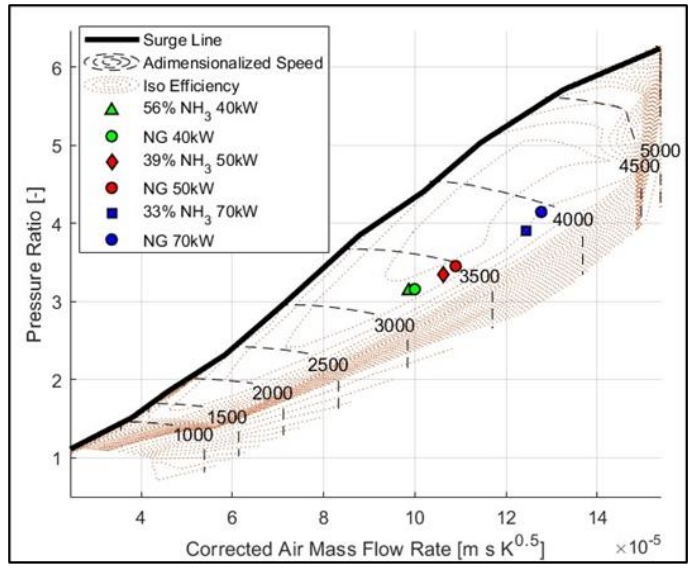

FIGURE 26: COMPRESSOR MAPS FOR DIFFERENT mGT POWER OUTPUT COMPARING PURE NATURAL GAS WITH THE MAXIMUM ACHIEVED AMMONIA-NG BLEND.

4 CONCLUSION

The experimental analysis on the T100 micro gas turbine, modified to operate with ammonia-natural gas blends, confirmed the feasibility and stability of using ammonia as a fuel. The results demonstrated that the mGT maintained stable operation and consistent power output under both steady-state and transient conditions, even with significant levels of ammonia injection.

Tests were conducted with mGT loads ranging from 100% to 43%, during which operational parameters such as fuel mass flow rates, injection pressure, rotational speed, temperatures, and pilot and main valve opening percentages were measured. Despite maintaining overall stability, the mGT experienced an efficiency decrease of approximately 2% when ammonia content was about 50% m/m. This aspect is mainly attributed to the lower c_p of the fuel mixture, but it is also affected by the low pressure ratio, air flow rate and rotational speed. Additionally, a significant temperature reduction in the pilot flame zone (-350°C to -380°C) was observed, indicating a decreased risk of flashback.

Significant findings included a marked reduction in CO_2 emissions, achieving up to 19.5% less compared to operation with natural gas alone. However, this benefit was accompanied by a substantial increase in NO_X emissions (2208 ppm with 50% m/m of ammonia), highlighting the necessity for incorporating an effective NO_X reduction system to ensure environmental compliance. Future study will also involve the measurement of CO.

Additionally, the formation of ammonium carbonate within the fuel lines, due to interactions between ammonia and CO_2 and H_2O present as impurities in the natural gas, was identified. This reaction led to reduced flow passage and subsequent pressure drops, impacting mGT performance. To mitigate this issue, it is recommended to pretreat natural gas to remove impurities or increase the mixing temperature to inhibit the formation of ammonium carbonate.

Detailed maps have been developed based on experimental results to characterize the mGT performance. It has been determined that operating with ammonia enables higher power output while maintaining improved compressor performance, consistently operating well away from the surge margin.

Overall, while integrating ammonia into the mGT fuel blend offers clear benefits for reducing carbon emissions without compromising the turbine stability, further efforts in emissions control and fuel system optimization are essential for ensuring long-term viability and compliance with environmental standards. The findings contribute valuable insights for future research and development in the field of sustainable power generation using carbon-free alternative fuels.

ACKNOWLEDGEMENTS

This project has received funding from the European Union’s Horizon 2020 research and innovation program under grant agreement No 884157 and from the Italian Ministry of University and Research under the National Recovery and Resilience Plan, Mission 4, Component 2, Investment 1.3, NextGenerationEU, Project “Network 4 Energy Sustainable Transition”, PE00000021, CUPJ33C22002890007.
This paper reflects only the authors' views and the Research Executive Agency and the European Commission are not responsible for any use that may be made of the information it contains.

REFERENCES

[1] Bäckstrand, K., Towards a Climate-Neutral Union by 2050? The European Green Deal, Climate Law, and Green Recovery, Routes to a Resilient European Union: Interdisciplinary European Studies, (2022) 39–61.
[2] Brzęczek, M., Kotowicz, J., Integration of alternative fuel production and combined cycle power plant using renewable energy sources, Applied Energy, 371 (2024) 123738.
[3] Raggio, M., Ferrari, M.L., Compressed air energy storage with T100 microturbines: Dynamic analysis and operational constraints, Journal of Energy Storage, 73 (2023) 109093_1-15.
[4] Veeraragavan, A., Montgomery, L. and Datas, A., 2014. Night time performance of a storage integrated solar thermophotovoltaic (SISTPV) system. *Solar energy*, *108*, pp.377-389.
[5] El-Maaroufi, A., Daoudi, M., Ahl Laamara, R., Optimal design and techno-economic analysis of a solar-wind hybrid power system for laayoune city electrification with hydrogen and batteries as a storage device, Physics and Chemistry of the Earth, 136 (2024) 103719.
[6] Bellotti, D., Rivarolo, M., Magistri, L., A comparative techno-economic and sensitivity analysis of Power-to-X processes from different energy sources, Energy Conversion and Management, 260 (2022) 115565.
[7] Clematis D, Bellotti D, Rivarolo M, Magistri L, Barbucci A. Hydrogen Carriers: Scientific Limits and Challenges for the Supply Chain, and Key Factors for Techno-Economic Analysis. *Energies*. 2023; 16(16):6035. https://doi.org/10.3390/en16166035
[8] Usman, M.R., Hydrogen storage methods: Review and current status, Renewable and Sustainable Energy Reviews, 167 (2022), 112743.
[9] Tiwari, S., Pekris, M.J., Doherty, J.J., A review of liquid hydrogen aircraft and propulsion technologies, International Journal of Hydrogen Energy, 57 (2024) 1174 – 1196.
[10] Bourzac, K., Carbon-free fuels could have a climatic dark side, Science, 382 (2023) 752.
[11] Staffell, I., Scamman, D., Abad, A.V., Balcombe, P., Dodds, P.E., Ekins, P., Shah, N., Ward, K.R., The role of hydrogen and fuel cells in the global energy system, Energy & Environmental Science, 12 (2019) 463-491.
[12] Cellek, M.S., The decreasing effect of ammonia enrichment on the combustion emission of hydrogen, methane, and propane fuels, International Journal of Hydrogen Energy, 47 (2022) 19916-19934.
[13] Wijayanta, A.T., Oda, T., Purnomo, C.W., Kashiwagi, T., Aziz, M., Liquid hydrogen, methylcyclohexane, and ammonia as potential hydrogen storage: Comparison review, International Journal of Hydrogen Energy: 44 (2019) 15026-15044.
[14] Wehrle, L., Ashar, A., Deutschmann, O., Braun R.J., Evaluating high power density, direct-ammonia SOFC stacks for decarbonizing heavy-duty transportation applications, Applied Energy, 372 (2024) 123646.
[15] Anfosso, C., Crosa, S., Iester, F., Bellotti, D. and Magistri, L., 2025. Investigation of an Ammonia-Fueled SOFC-mGT Hybrid System: Performances Analysis and Comparison With Natural Gas-Based System. *Journal of Engineering for Gas Turbines and Power*, *147*(5).
[16] Romano, C., Bellotti, D., Pucci, E., Fadlun, E., Roma, M., Ghezzi, S., Manferino, G., Anfosso, C. and Monacchini, C., 2024, September. Ammonia Cracking As Auxiliary System for Gas Turbine: Preliminary Studies. In *ASME Power Conference* (Vol. 88186, p. V001T03A003). American Society of Mechanical Engineers.
[17] Olivier Herbinet, Pietro Bartocci, Alon Grinberg Dana, On the use of ammonia as a fuel – A perspective, Fuel

Communications, Volume 11,2022, 100064, ISSN 2666-0520, https://doi.org/10.1016/j.jfueco.2022.100064.

[18] Ayman M. Elbaz, Shixing Wang, Thibault F. Guiberti, William L. Roberts, Review on the recent advances on ammonia combustion from the fundamentals to the applications, Fuel Communications, Volume 10, 2022, 100053, ISSN 2666-0520, https://doi.org/10.1016/j.jfueco.2022.100053.

[19] Shimura, J.H., Masayasu, S., Kurata, O., Ekenechukwu Chijioke, O., Hirofumi, Y., Takahiro, I., Taku, T., Norihiko, I., Yong, F., Combustion and Emission Characteristics of an Ammonia Micro gas Turbine Combustor With a Twin-Fluid Atomizer, Journal of Engineering for Gas Turbines and Power, 146 (2024) 111001.

[20] Zhang X, Wang J, Chen Y, Li C. Effect of CH4, Pressure, and Initial Temperature on the Laminar Flame Speed of an NH3-Air Mixture. ACS Omega. 2021 May;6(18):11857-11868. DOI: 10.1021/acsomega.1c00080. PMID: 34056340; PMCID: PMC8154007.

[21] A. Valera-Medina, S. Morris, J. Runyon, D.G. Pugh, R. Marsh, P. Beasley, T. Hughes, Ammonia, Methane and Hydrogen for Gas Turbines, Energy Procedia, Volume 75, 2015, Pages 118-123, ISSN 1876-6102, https://doi.org/10.1016/j.egypro.2015.07.205.

[22] Douglas, C. M., Martz, T. D., Steele, R. C., Noble, D. R., Emerson, B. L., and Lieuwen, T. C. (October 17, 2023). "Pollutant Emissions Reporting and Performance Considerations for Ammonia-Blended Fuels in Gas Turbines." ASME. *J. Eng. Gas Turbines Power*. January 2024; 146(1): 011003. https://doi.org/10.1115/1.4063417

[23] Heggset, T, Meyer, O, Gruber, A, Tay-Wo-Chong, L, & Ciani, A. "Numerical Assessment of a Rich-Quench-Lean Staging Strategy for Clean and Efficient Combustion of Partially Decomposed Ammonia in the Constant Pressure Sequential Combustion System." *Proceedings of the ASME Turbo Expo 2023: Turbomachinery Technical Conference and Exposition*. *Volume 3B: Combustion, Fuels, and Emissions*. Boston, Massachusetts, USA. June 26–30, 2023. V03BT04A057. ASME. https://doi.org/10.1115/GT2023-103835

[24] Avila, C.D., Cardona, S., Abdullah, M., Younes, M., Jamal A., Guiberti T.F., Roberts W.L., Experimental assessment of the performance of a commercial micro gas turbine fueled by ammonia-methane blends, Applications in Energy and Combustion Science, 13 (2023)100104.

[25] Arai, K., Kawano, M., Kudomi, N., Sugiura, H., Yasui, Y., Ishiwaki, F. (2023). Development of 300 kW Ammonia Combustion Micro Gas Turbine. In: Aika, Ki., Kobayashi, H. (eds) CO2 Free Ammonia as an Energy Carrier. Springer, Singapore. https://doi.org/10.1007/978-981-19-4767-4_34

[26] Horizon Europe FLEXnCONFU Project https://flexnconfu.eu/ (last access: 23rd October 2024).

[27] Rossi, I. and Traverso, A., 2018. Ambient temperature impact on micro gas turbines: experimental characterization. *Acta Polytechnica CTU Proceedings*, *20*, pp.78-85.

[28] Ferrari, M.L., Rossi, I., Sorce, A., Massardo A.F., Advanced Control System for Grid-Connected SOFC Hybrid Plants: Experimental Verification in Cyber-Physical Mode, Journal of Engineering for Gas Turbines and Power, 141 (2019) 091019.

[29] Pascenti, M., Ferrari, M.L., Magistri, L., Massardo, A.F., Micro Gas Turbine Based Test Rig for Hybrid System Emulation, Paper n. GT2007-27075, ASME Turbo Expo 2007, Montreal (Canada) (2007).

[30] Bellotti, D., Anfosso, C., Magistri, L., Massardo A.F., Partially cracked ammonia for micro-Gas Turbine application, Paper n. GT2023-105386, ASME Turbo Expo 2023, Boston (Massachusetts) (2023).

[31] Bonasio, V. and Ravelli, S., 2022. Performance analysis of an ammonia-fueled micro gas turbine. *Energies*, *15*(11), p.3874.

[32] Osamu Kurata, Norihiko Iki, Takayuki Matsunuma, Takahiro Inoue, Taku Tsujimura, Hirohide Furutani, Hideaki Kobayashi, Akihiro Hayakawa, Performances and emission characteristics of NH3–air and NH3CH4–air combustion gas-turbine power generations, Proceedings of the Combustion Institute, Volume 36, Issue 3, 2017, Pages 3351-3359, ISSN 1540-7489, https://doi.org/10.1016/j.proci.2016.07.088.

[33] Normativa Gas, Decreto ministeriale 18 maggio 2018 - Gas combustibile, aggiornamento regola tecnica, Ministero dello Sviluppo Economico, 2018, Available Online: https://www.mimit.gov.it, Accessed: November 2024

